Error Analysis for Vertical Test Stand Cavity Tests at Fermilab

Alex Melnychuk

Fermilab, Batavia, Illinois

September 17, 2013

Uncertainty calculations for Q_0 and E_{acc} measurements at Vertical Test Stand (VTS) facility at IB1 at Fermilab are discussed. Sources of uncertainties and assumptions on their correlations are reviewed. VTS hardware components with non-negligible instrumental errors are discussed. Relative contributions of individual sources to the total uncertainties are assessed. Comparisons with previous publications on the subject are made. Stability of VTS test results with respect to potential mismeasurements of calibration coefficients and decay constant are studied.

Total uncertainties were estimated to be at the level of approximately 4% for both Q_0 and E_{acc} for input coupler β_1 in the interval between 0.5 and 2.5 and rising with β_1 outside this interval. The results were found to be much more sensitive to the treatment of correlations than to variations in the accuracy of power level measurements and operator error.

Plans for overall improvement of uncertainty estimation accuracy and possibility of reducing Q_0 uncertainty due to τ_L are discussed. Attempts to derive Q_0 vs. E_{acc} from decay measurement alone are described.

Changes since December 5, 2012 version

- added note number
- change version number from 0.2 to 1.0
- commented out controversial proposal to include the difference between low power amplifier and high power amplifier measured Q_{ext2} as additional systematic error

Changes since August 28, 2012 version

- extended footnote about assumptions on correlation of uncertainties associated with variations in cable losses after cable heating
- mention in the footnote that `uncertainties` package relies on *linear* error propagation theory but linearity assumption is likely to break down at high β_1, quick estimates suggest that with β_1=40 we may be getting into non-linear regime
- error on kappa 1% conservative estimate of one standard deviation (Timergali Khabibouline)
- instabilities when Q is very high approaching 10E+11(and especially when beta1 is close to 1 ?) (takes long to fill up, takes much time to reach equilibrium b/w incident and reflected power, there could be larger uncertainties in such case
- added short section to describe plans for further improvement of error analysis: 1) take into account leakage of P_i into P_r signal inside directional coupler (info from TD T&I colleagues) and 2) come up with point-to-point invariant quantities (Q1?) and obtain error estimate from their spread and/or difference between decay and CW measurement

Contents

1 Brief Overview of VTS Measurement

VTS measurement consists of three main stages:

1. **Cable calibrations.** Calibration coefficients C_i, C_r, C_t are measured. These coefficients relate incident, reflected[1], and transmitted power levels between VTS stand power meter readings and actual power levels at the cavity input coupler and output coupler ports inside the dewar. Overview of calibration procedure as well as derivation of formulas for C_i, C_r, and C_t can be found in Appendix A.

2. **Field probe calibration** (also referred to as "decay measurement"). Output coupler (field probe) quality factor Q_{ext_2} is measured at this stage.

3. **Measurement of Q_0 and E_{acc}** (also referred to as "CW measurement").

At each of the three stages measurements of power levels are performed with the same power meters[2]. Therefore strong correlations between quantities measured at each stage are expected and should be properly taken into account. Relationships between these three stages can be understood from the diagram shown in Fig. 1. Note that formulas in this diagram are taken from [1]. Corresponding formulas in the main body of this reference contain errors. Both decay measurement and CW measurement rely on cable calibration coefficients measured at stage 1. CW measurement relies on Q_{ext_2} established in the decay measurement.

2 Uncertainties to be propagated

Sources of uncertainties in Q_0 and E_{acc} include:

- finite precision and sensitivity limit of power meters;
- dependence of cable losses on power level;
- operator error;
- uncertainty in measured decay constant τ_L.

Note that in Fig. 1 we can see two quantities that are used in the calculations but not mentioned above among the sources of uncertainties. These are the RF drive frequency at cavity resonance and $\varkappa$. Frequency is measured with very high precision with Agilent 53132A frequency counter, its frequency resolution is up to 12 digits in one second [2] and the RF source (Agilent E4422B) has frequency resolution of 0.01Hz [3]. $\varkappa$ is taken from the simulations[3].

[1] Here and in the rest of this document by "reflected power" we mean the power that travels in the direction opposite to incident power, including both the signal reflected from the cavity and the signal which leaks out of the cavity through input coupler

[2] at the calibration stage additional portable power meter is used

[3] Note that `r/Q` that appears in the formula inside "CW Measurement" box is per unit of length (expressed in Ω/m). At the same time, `r/Q` that appears on the bottom left of the diagram below "CW Measurement"

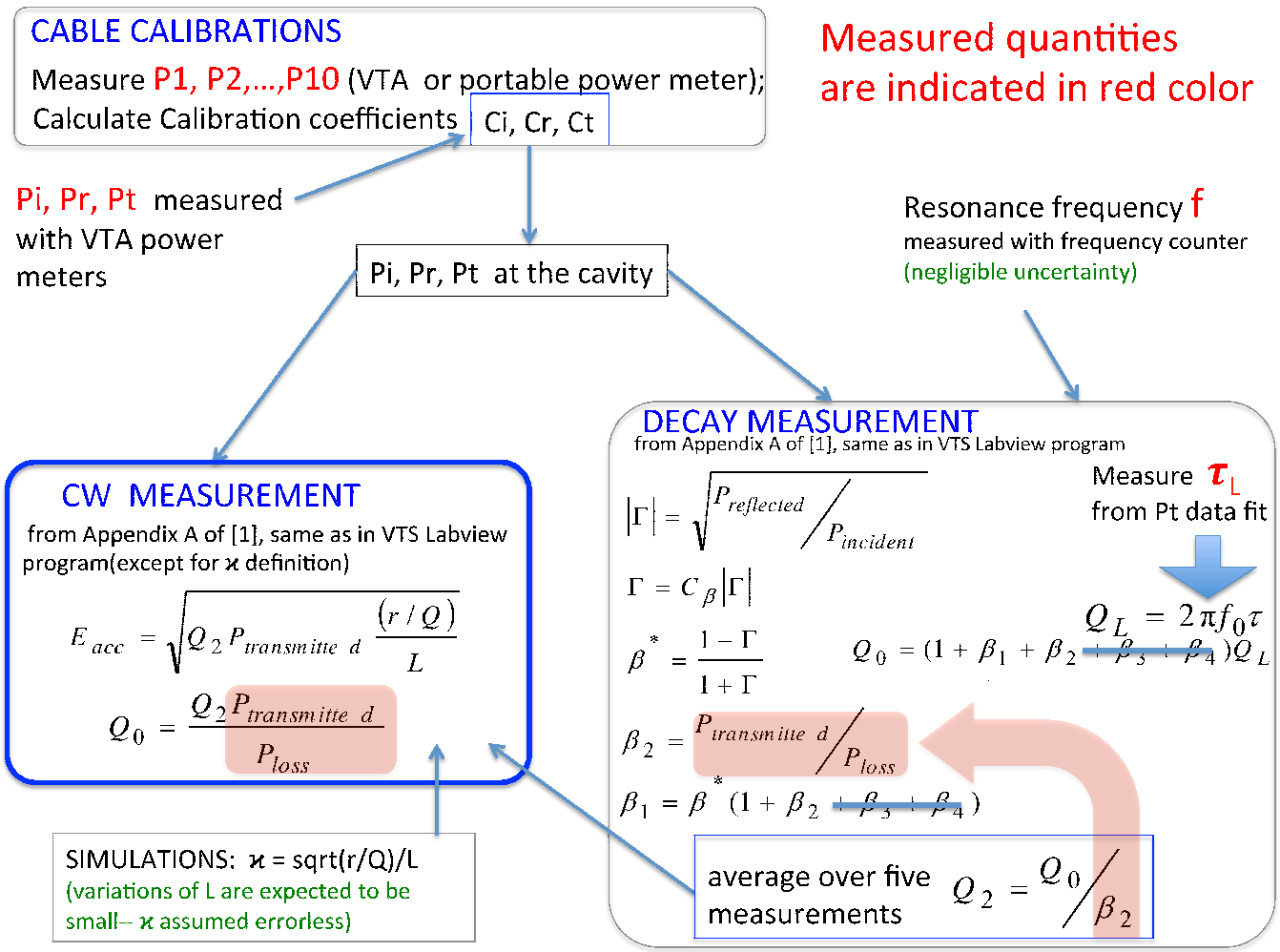

Figure 1: VTS test layout.

2.1 Power Meters

Currently three power meters are used at VTS stand (incident, reflected, and transmitted power) and a portable power meter for cable calibrations. These devices are Agilent E4419B (or E4418B in case of transmitted power) power meters, which use E9301A sensor heads[4]. The following errors should be considered:

1. power meter accuracy of 0.5% [6];
2. sensor non-linearity of 4% [7];
3. sensor calibration uncertainty of 1% [8].

Adding all of the above in quadrature gives total combined precision of a power meter and sensor of 4.2%. Sensitivity limit of 9301A sensor heads is 1nW [9]. More information on evaluating power meter and sensor head precision can be found in [10].

2.2 Cable Losses

Cable losses inside the dewar, in general, depend on the power level supplied to the cavity[5].

According to reference [11] after tens of Watts are applied to a cable, cable losses are not stable[6] (due to variations in impedance mismatches as the cable warms up ?). We estimate the size of the effect of power level dependence, using available VTS data from 1.3GHz 9-cell and 325MHz SSR1 cavity tests. This approach is attractive because results are extracted from exactly the same setup as during VTS tests, including temperature conditions and presence of other components e.g. directional, couplers, connectors, and cables outside the dewar. We made use of Calibration Step 8, which is included in the standard VTS test procedure as minimal re-calibration of cables as the test progresses. We compared the values of calibration coefficients before and after this re-calibration and estimated the variation to be 5% for C_i and C_r (no variation for C_t) [12].

2.3 Operator Error

By "operator error" we mean the following causes of C_i, C_r, C_t variations:

- tightness of cable connections by operator A is more uniform throughout the steps of the calibration procedure than by operator B;

box is expressed in Ω. The latter choice is consistent with the values of $\varkappa$ provided as input to VTS LabView program i.e. 30.919, 88.4735, and 115.2 for 1.3GHz 9-cell, 1.3GHz 1-cell, and 325MHz single spoke cavity respectively. Here 325MHz cavity $\varkappa$ value of 115.2 is based on ANL definition of effective length $L_{eff}=2/3\beta\lambda$ (L_{eff}=135mm, r/Q=242Ω), therefore VTS results may need to be rescaled to a more modern definition of effective length ($L_{eff}=\beta\lambda$). More info can be found in [4].

[4]note that reference [5] mentions different sensor head type

[5]In principle, cable losses depend also on signal frequency. Signal attenuation due to ohmic losses in the conductors ($\propto \sqrt{f}$) and in the dielectric($\propto f$) as well as signal reflections due to impedance mismatches (impedance depends on f) contribute to this dependence. Reference [13] indicates cable loss variations of up to 6% per 1MHz change at 805MHz. However, in IB1 VTS setup, this dependence turns out to be negligible

[6]Cable loss variations of up to ≈15% at 50W are possible. However, these observations were not made on Times Microwave cables, which are used in VTS1 in IB1.

- RF power may drift slightly, hence operator-dependent delay between taking a measurement and entering it into the calibration program introduces some error;
- any random error that has to do with variations in hardware configuration e.g. bending of the cables.

On the other hand, large shifts in calibration coefficients due to abnormal hardware conditions e.g. faulty connector should be treated separately, they do not fall under "operator error" category. Based on current experience, we set 3% upper bound on operator error [14].

2.4 Decay Constant Uncertainty

2.4.1 Measurement of Decay Constant

Decay Constant τ_L is determined from a fit to $P_{transmitted}$ signal after RF power is turned off when cavity is at resonance. Measurement is performed at E_{acc} in the range between 3 and 5 MV/m. Exponentially decaying $P_{transmitted}$ signal is sampled with crystal detector (low barrier Schottky diode detector) Agilent 8472B. Signal sampling is performed every two milliseconds for six seconds from the moment at which RF power is turned off. The data are fit with the exponential function. Lower edge of the fitting range corresponds to the moment at which RF power is turned off (when $P_{transmitted}$ signal is at maximum). The upper edge of the fitting range corresponds to the moment at which $P_{transmitted}$ signal decayed to 95% of its maximum value. We considered the following errors in the decay measurement:

1. Instrumental error in crystal detector.
2. Fit error.
3. Error due to Q-slope.

2.4.2 Instrumental Error in Crystal Detector

In general, crystal detector can produce three types of errors: constant offset, non-linearity, and random noise. Constant offset applied to all points in the fit range would not affect the decay slope.

Non-linearity, in contrast, would have an effect on the decay slope. We double-checked that $P_{transmitted}$ VTS electronics circuit keeps Agilent 8472B detector in the linear regime, details can be found in Appendix A.

Random noise from crystal detector together with noise from any other conceivable source (e.g. helium vapor pressure fluctuations affecting capacitance of the cavity) contributes to fit error.

2.4.3 Fit Error

First we estimated the spread of $P_{transmitted}$ data points by subtracting fit function from the data during the first 100 msec (TE1PAV002 VTS test on 05/15/12). The range was chosen to be small enough so that the data points scatter around the fit line but do not deviate systematically from the fit (due to Q-slope). We estimated the spread to be 4%. This error

was assigned to all data points during the fit and the corresponding fit error on τ_L was found to be 2%. We conservatively use 3% as an estimate of τ_L fit error[7]. Additional information can be found in [15].

We studied possibility of reducing τ_L fit error by extending the fit range. In doing so one needs to be careful not to introduce large error due to Q-slope, which is described in the next section. τ_L error comparisons for different fit ranges can be found in [18].

It is possible to bring τ_L fit error below 1%. Such reduction in error may become important if very precise VTS measurements are needed. Note that τ_L error reduction would lead to CW Q_0 error reduction only for β_1 near 1. When β_1 is large Q_0 error is dominated by P_{loss} error, hence reduction in τ_L error is immaterial. In contrast, E_{acc} error will be noticeably reduced as a consequence of τ_L error reduction at any β_1.

2.4.4 Error due to Q-slope

Decay constant τ_L depends on three quality factors: Q_{ext1}, Q_{ext2}, and intrinsic Q_0. If at least one of these three quantities changes during decay measurement the decay would no longer be described by a simple $\propto \exp -t/\tau_L$ function since τ_L itself becomes a function of time. Such dependence introduces an ambiguity in τ_L measured under the assumption of simple exponential decay. Since Q_{ext1} and Q_{ext2} depend only on the geometry of the cavity and on the position of the antennas, their values remain fixed throughout a VTS test. Q_0, on the other hand, depends on E_{acc}. In the presence of strong Q_0 vs. E_{acc} dependence in the [3, 5] MV/m interval (Low Field Q-Slope) where the decay measurement is performed additional uncertainty may need to be ascribed to τ_L to take into account aforementioned ambiguity. We estimated the size of the uncertainty by modeling τ_L measurement under two extreme Q-slope scenarios: 1) flat Low Field Q-slope and 2)Q_0 increase by a factor of 2 between 0 and 5 MV/m. We concluded that τ_L error due to Q-slope is negligible. This conclusion is valid for fitting range between maximum and 95% (range that is currently in use) or smaller fitting range. Details of our studies can be found in [16].

2.4.5 Summary of τ_L Error

τ_L error is of statistical nature and is equal to 3%.

2.5 Uncertainty on $\varkappa = \sqrt{r/Q}/L$

Parameter $\varkappa = \sqrt{r/Q}/L$, which is used for calculating E_{acc}, is estimated from the simulations. The simulations assume perfect cavity geometry. Deviation of tested cavity geometry from perfect geometry translates into uncertainty in $\varkappa$. Size of this uncertainty can be conservatively estimated as 1% (standard deviation) [17]. Since this uncertainty is small and not correlated with other uncertainties, when added in quadrature, it changes the total uncertainty by negligible amount. Therefore it was not propagated.

[7] Using tools developed for estimating fit error we also attempted to extract Q_0 vs E_{acc} curve from the decay measurement alone. This effort is described in Appendix E.

Source	Uncertainty	LabView VTS program settings
Power meter sensitivity	1nW	1nW
Power meter precision	4.2%	2%
Operator error	3%	not propagated
Cable losses	5% (C_i and C_r), 0% (C_t)	not propagated
C_i, C_r, C_t	15.5%, 8.9%, 6.7% *(these errors are not treated as coming from independent source, they result from propagating errors from the four sources above)*	7.5% (constant for all coefficients, treated as independent source)
Decay constant	3%	3%

Table 1: Uncertainties which are propagated into Q_0 and E_{acc} uncertainties in CW measurement. Middle column shows recently estimated uncertainties which are described in this document. Right column shows corresponding uncertainties used by LabView VTS program.

2.6 Summary of Uncertainties to be Propagated

Uncertainties used in Q_0 and E_{acc} error propagation are summarized in Table 1. The table also shows comparison with corresponding uncertainties used by LabView VTS program for error propagation on Q_0 and E_{acc}.

3 Correlations

When propagating errors on CW measured Q_0 and E_{acc} it is important to take into account the correlation between the three stages of the VTS measurement (cable calibration, decay measurement, and CW measurement). This correlation arises from using the same devices (power meters) for power level measurements at each of the three stages. To be more precise, same $P_{incident}$ power meter is used for measuring incident power level at each stage, same $P_{reflected}$ power meter is used for measuring reflected power level at each stage, and same $P_{transmitted}$ power meter is used for measuring transmitted power level at each stage. These three power meters are located at the VTS test stand[8].

We assume that the same physical device mismeasures power level by the same fractional amount whenever it is used throughout a given VTS test. In other words, error on $P_{incident}$, for example, measured during cable calibrations will be 100% correlated with the error on $P_{incident}$ measured in the decay measurement (or/and CW measurement). Measurement errors on physically distinct devices, on the other hand, are assumed to have zero correlation regardless of whether the measurements are made during the same stage or at different stages of the VTS test.

C_i, C_r, and C_t errors are by definition 100% correlated between decay measurement and

[8]There is also fourth, portable, power meter, which is used only during cable calibrations and does not bring any correlation.

CW measurement since same cable calibration is applied in both cases[9]

Outlined treatment of correlations is quite different from that adopted in LabView VTS program (based on [1]). Treatment of correlations employed by VTS LabView program is summarized in Appendix F.

4 Procedure for Error Analysis

Our error analysis procedure consists of several steps:

1. Based on the VTS data contained in the VTS test output file (uncorrected power levels, calibration coefficients C_i, C_r, C_t, τ_L, frequency) reproduce central values of Q_{ext2} from decay measurement and Q_0, E_{acc} from CW measurement. Offline calculations are performed with `python` scripts.

2. Extend previous step to calculation of uncertainties: reproduce uncertainties on Q_{ext2}, Q_0, and E_{acc}. At this stage we use same values of uncertainties (of individual sources) to be propagated and same assumptions on their correlations as in LabView VTS program[10]. Calculations start with uncorrected power levels and C_i, C_r, C_t values from VTS data file. No data from cable calibration measurements are used at this step. Error propagation is performed within the framework of `uncertainties` software package [19] in which, at this step, most of the correlations are deliberately turned off to conform to VTS LabView program treatment of correlations[11].

3. Modify assumptions on correlations[12] and turn on corresponding correlations within `uncertainties` framework. Unlike in previous step, here we calculate C_i, C_r, and C_t (and propagate errors) starting with power level measurements taken at the stage of cable calibrations[13].

[9]However, in principle, one can argue that cable loss error part of the calibration error should be taken into account only for CW measurement when large amount of power goes through the cable but not for decay measurement when RF power level is relatively small. Adopting this point of view would also have implications for treatment of correlations. In that case C_i and C_r errors will be less than 100% correlated between decay and CW measurement (with cable loss error not present in the decay measurement). We decided to leave this detail out of the analysis for the purposes of simplicity, keeping in mind that general strategy of current error analysis was to make conservative error estimates for each source. Therefore significant under-estimation of Q_0 and E_{acc} error due to exaggerated C_i and C_r correlation between decay and CW is not expected.

[10]LabView VTS program uncertainty settings can be found in the right column of Table 1 in Section 2.6. Treatment of correlations employed by VTS LabView program is summarized in Appendix F.

[11]`uncertainties` package introduces a data type which carries a central value and associated uncertainty. An expression built out of variables of such type has the same type. Its associated uncertainty is a result of propagation of errors on variables that enter the expression. When such expressions are further combined into more complicated expressions `uncertainties` keeps propagating the errors keeping track of correlations between variables throughout all the steps of the calculation. Note that `uncertainties` package relies on *linear* error propagation theory but linearity assumption is likely to break down at high β_1. Quick estimates suggest that with β_1 around 40 we may be already getting into non-linear regime.

[12]Modified assumptions on correlations are described in Section 3.

[13]These data are not part of the standard VTS output file, they were recorded by hand during actual cable calibration for the VTS test picked for verification of offline error analysis tools

4. Replace values of uncertainties to be propagated with our estimates (listed in Section 2.6).

5. Re-calculate uncertainties on Q_{ext2}, Q_0, and E_{acc}.

5 Results

Figure 2 shows our offline estimated fractional errors on Q_0 and E_{acc} as a function of E_{acc} (right column) as well as corresponding errors calculated by LabView VTS program (left column). Our offline estimated errors are significantly lower than those from LabView VTS program because in the former case correlations are taken into account, which leads to large cancellations of common errors. Let us point out several noteworthy features of the plots in the right column in Fig. 2.

- Very large errors at very low E_{acc} correspond to measurements taken with very low RF power so that power meter sensitivity threshold starts contributing significantly to the total fractional error.

- Red curve on the top right plot is not visible because it is covered by the blue curve. In other words, cable calibration errors that originate from cable losses and operator error, when propagated, do not add significantly to cable calibration errors that originate from finite power meter precision. This would not be so if the correlations were not taken into account as demonstrated in [26].

- In general, one might expect total E_{acc} error to be smaller by a factor of 2 than total Q_0 error due to a square root in the E_{acc} expression. However, because CW calculations are essentially three step calculations with correlations such simple rule no longer applies.

- Relative impact of including τ_L error (black curve compared with blue curve) is much more significant for Q_0 than for E_{acc}. This is at least in part related to square root E_{ecc} dependence on τ_L versus Q_0 linear dependence on τ_L mentioned in the previous bullet. The τ_L dependence comes via Q_2 and the error on τ_L is not correlated with any other errors involved in error propagation.

- E_{acc} errors do not depend on E_{acc}, which can be understood from the analysis of the E_{acc} formula in the CW measurement box of the diagram in Fig. 1. The two quantities that contribute uncertainties to the total E_{acc} uncertainty are Q_2 and $P_{transmitted}$. Note that fractional errors on both of these quantities remain fixed at any CW measurement point. Q_2 is determined in the decay measurement and then used in the CW measurement, hence its fractional error does not depend on CW E_{acc}. $P_{transmitted}$ fractional error depends on fixed power meter precision and on operator error during calibration, hence no dependence on E_{acc} either.

- Q_0 errors, in contrast with E_{acc} errors, depend on E_{acc}. The origin of this dependence can be traced to the dependence of P_{loss} fractional error on RF power coupling β_1, defined as a ratio of intrinsic quality factor to input coupler quality factor Q_0/Q_1.

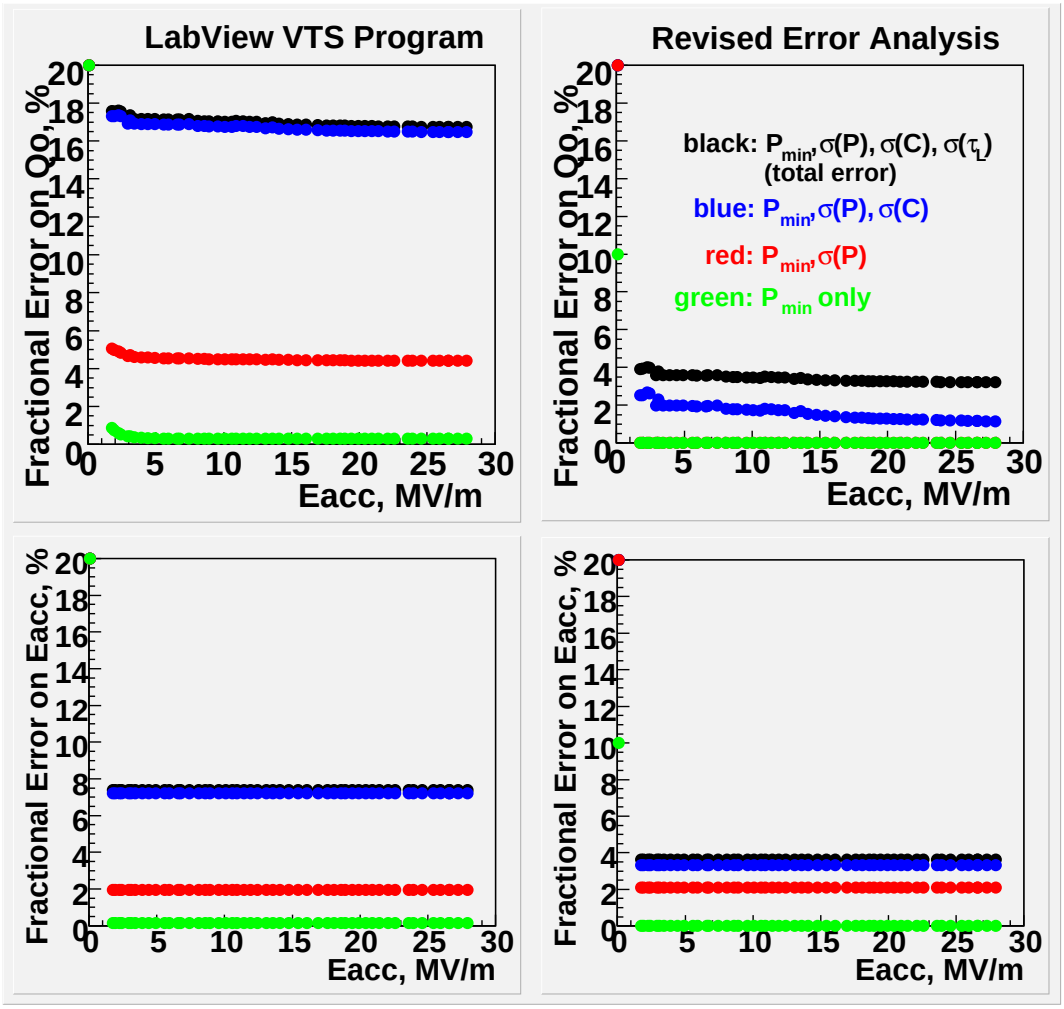

Figure 2: Fractional errors on Q_0 and E_{acc} as a function of E_{acc}. Left column: errors from LabView VTS program. Right column: offline estimated errors. Top row: Q_0 errors. Bottom row: E_{acc} errors. Green: only power meter sensitivity limit is included in the errors that are propagated. Red: finite power meter precision is included in addition to sensitivity limit. Blue: cable loss error and operator error are included in addition to power meter sensitivity limit and finite precision. Black: τ_L error included in addition to all errors mentioned above. The data used in the calculations comes from 2K VTS test of TB9NR004 cavity performed in March 2012.

Figure 3 shows dependence of P_{loss} and Q_0 fractional errors on β_1 in CW measurement for two VTS tests. As β_1 increases, values of $P_{reflected}$ and $P_{incident}$ become closer to each other making P_{loss} smaller, therefore P_{loss} fractional error grows. P_{loss} error, when propagated, brings dependence on β_1 into Q_0 error as well. Generally, as E_{acc} increases, Q_0 decreases. Therefore $\beta_1 = Q_0/Q_1$ decreases, which in turn leads to decrease of Q_0 error manifested on the top right plot in Fig. 2.

E_{acc} error in CW measurement does not vary with β_1 due to the reasons discussed in the previous bullet. However the size of constant E_{acc} error in CW measurement depends on β_1 in the decay measurement.

6 Summary

Uncertainties contained in the VTS data files calculated by LabView VTS program appear to be significantly overestimated due to incomplete treatment of correlations[14]

Fractional Q_0 and E_{acc} uncertainties can be both approximated by constant 4% uncertainty reasonably well for values of β_1 below 2.5. For higher values of β_1 Figure 3 of this document can be used for guidance on the expected size of the uncertainty. For accurate estimates of uncertainty `python` scripts mentioned in this document should be used.

Naturally conclusions of our error analysis are tied to the list of sources of error that we considered and claim to understand. Additional non-negligible sources of uncertainty of which we are unaware at the moment may also contribute. In particular, instabilities in the electronics may contribute to overall uncertainty in a way that does not allow rigorous quantification. For example, a known drift of RF source power level at a fixed attenuation, in principle, may have consequences for the measurement of τ_L. Instabilities in the feedback loop system may invalidate "peak of the resonance" assumption when a measurement point is taken leading to miscalculation of β_1 and, consequently, Q_{ext2}. Additional instabilities arise in special cases when Q is very high (approaching 10E+11)[15]. Since in this case, due to long fill-up time, equilibrium between incident and reflected power is reached very slowly and it is not stable.

We also compared sensitivity of Q_0 and E_{acc} CW measurements to measurements of C_i, C_r, C_t, and τ_L (Appendix C). We found largest sensitivity to τ_L (simple linear and square root dependence for Q_0 and E_{acc} respectively) and practically no sensitivity to C_t.

7 Plans for Improvement of Error Analysis

7.1 Uncertainty from Directional Coupler

Cable calibration procedure described above as well as calculations of Q_0 and E_{acc} assume that directional coupler provides a perfect separation of P_i and P_r signals based on the

[14]This implies, that for the purpose of proper estimation of Q_0 and E_{acc} CW errors it is not necessary to perform averaging of Q_{ext2} error since this error is an ingredient in the procedure which leads to exaggerated error on Q_0 and E_{acc}. A note on the validity of averaging procedure itself can be found in Appendix D.

[15]especially when β_1 is close to 1?

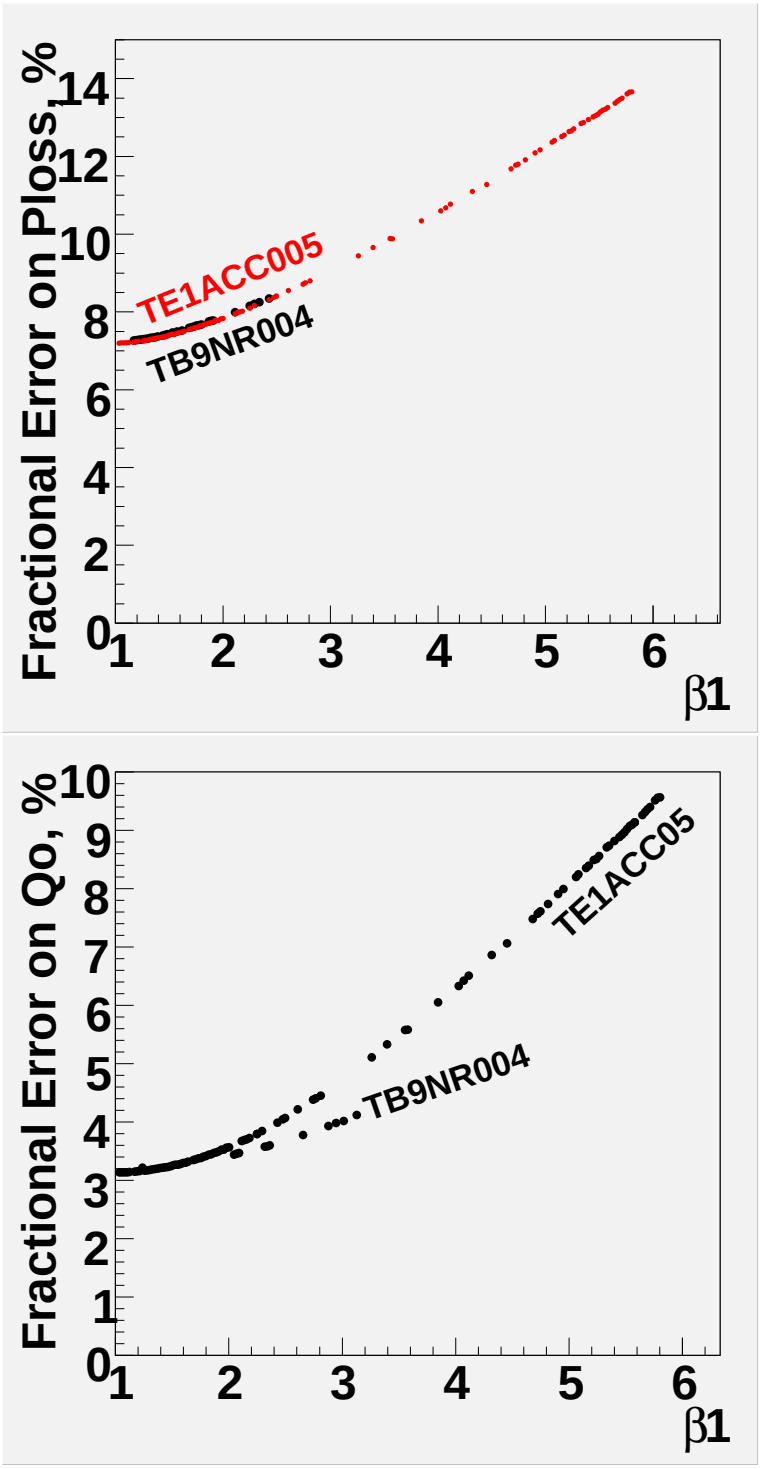

Figure 3: Top: β_1 dependence of P_{loss} fractional error in CW measurement. Two tests are shown: 03/12 TB9NR004 2K test(black) and 05/12 TE1ACC005 test in which temperature was lowered below 2K(red). Bottom: β_1 dependence of Q_0 fractional error in CW measurement for the same two VTS tests. Faster Q_0 error growth in case of TE1ACC005 could be due to larger β_1 in the decay part of the test or related non-trivial dependence of error on other quantities involved in error propagation.

direction of signal travel. In reality some fraction of P_i signal leaks into P_r pick up probe and vise versa. Such ambiguity ultimately limits the accuracy with which Q_0 and E_{acc} can be measured. The amount of leakage should be quantified and included in the error analysis.

8 Appendix A: Cable Calibration Procedure

Cable calibration procedure consists of five steps[16], summarized in Fig. 4, in which ten power level measurements are taken. We label them as P_1, P_2,...,P_{10} following convention in [27]. Using these measurements cable calibration coefficients C_i, C_r, and C_t are obtained as follows.

As mentioned in Section 1 our goal is to find power signals at the cavity, i.e. incident power ($P_{incident}$) and reflected power ($P_{reflected}$) at point D and transmitted power ($P_{transmitted}$) at point A based on the signals measured by power meters at VTA (VTS test area).

$$P_{incident}@D = C_i \times P_{incident}@VTA \tag{1}$$

$$P_{reflected}@D = C_r \times P_{reflected}@VTA \tag{2}$$

$$P_{transmitted}@A = C_t \times P_{transmitted}@VTA \tag{3}$$

Power levels at the LHS of the above equations can be referred to as corrected power levels, whereas those at the RHS as uncorrected power levels.

First we set an intermediate goal: write down signals at the points on the top plate (points E and B respectively). Let us denote by (P_X-P_Y) amplification of signal in dB as it travels from point X to point Y. Let (P_X-P_Y) by our convention be a positive number. Then "-(P_X-P_Y)" is attenuation in dB, a negative number. Then power levels and points E and B can be expressed as

$$P_{incident}@E = P_{incident}@VTA + (P_5 - P_6) \tag{4}$$

$$P_{reflected}@E = P_{reflected}@VTA + (P_7 - P_8) \tag{5}$$

$$P_{transmitted}@B = P_{transmitted}@VTA + (P_2 - P_1) \tag{6}$$

First we focus on point E and relate $P_{incident}@E$ with $P_{reflected}@E$:

$$P_{incident}@E - 2(P_D - P_E) = P_{reflected}@E \tag{7}$$

where -(P_D-P_E) is a one way cable loss as signal travels from E to D. -2(P_D-P_E) is a two way cable loss as signal travels from E to D and back from D to E. In (7) we rely on assumption that the cavity is off the resonance (i.e. we have open circuit), so that all incident power that arrives at the cavity gets reflected back.

Now let us relate (P_D-P_E) to power measurements during cable calibrations. Substitute RHS of (4) and RHS of (5) in place of $P_{incident}@E$ and $P_{reflected}@E$ in (7) to obtain

$$P_{incident}@VTA + (P_5 - P_6) - 2(P_D - P_E) = P_{reflected}@VTA + (P_7 - P_8) \tag{8}$$

[16] in the absence of HOM couplers

In (8) substitute P_9 and P_{10} from Step 8 for $P_{incident}@VTA$ and $P_{reflected}@VTA$ respectively to obtain

$$P_9 + (P_5 - P_6) - 2(P_D - P_E) = P_{10} + (P_7 - P_8) \tag{9}$$

From (9) we obtain expression for "-(P_D-P_E)":

$$-(P_D - P_E) = (P_{10} - P_9 + P_7 - P_8 + P_5 - P_6)/2 \tag{10}$$

Having obtained expression for "-(P_D-P_E)" in terms of power levels measured during calibration we can calculate incident and reflected power levels at point D. Let us start with incident power.

$$P_{incident}@D = P_{incident}@E - (P_D - P_E) \tag{11}$$

In (11) substitute for $P_{incident}@E$ RHS of (4) and for "-(P_D-P_E)" RHS of (10) to obtain

$$P_{incident}@D = P_{incident}@VTA + (P_{10} - P_9 + P_7 - P_8 + P_5 - P_6)/2 \tag{12}$$

Second term in (12) is C_i expressed in dB i.e. $C_i = (P_{10} - P_9 + P_7 - P_8 + P_5 - P_6)/2$.

Now repeat the last argument for reflected power.

$$P_{reflected}@D = P_{reflected}@E + (P_D - P_E) \tag{13}$$

Note the plus sign in between two terms in RHS of (13). It implies that reflected power level at point D was higher than it was at point E after it traveled from D to E (reflected power signal travels from D to E i.e. away from the cavity). This point about plus sign is important. If we change the plus sign to minus in (13) i.e. flip the direction of travel of the reflected signal then we'll eventually arrive at the formula for C_r in [28] which, in our opinion, appears to be incorrect. In (13) we substitute for $P_{reflected}@E$ RHS of (5) and for (P_D-P_E) RHS of (10) taken with the opposite sign to obtain

$$P_{reflected}@D = P_{reflected}@E + (P_7 - P_8 - P_{10} + P_9 - P_6 + P_5)/2 \tag{14}$$

Second term in (14) is C_r expressed in dB i.e. $C_r = (P_7 - P_8 - P_{10} + P_9 - P_6 + P_5)/2$. Note that our derived expression for C_r does not agree with that in [28]. We think this may be related to a specific assumption made in [28] as explained above. Our expression is in agreement with LabView VTS program calculation.

Remaining coefficient is for transmitted power.

$$P_{transmitted}@A = P_{transmitted}@B + (P_3 - P_4)/2 \tag{15}$$

Then use equation (16) for $P_{transmitted}@B$ to obtain

$$P_{transmitted}@A = P_{transmitted} + (P_2 - P_1) + (P_3 - P_4)/2 \tag{16}$$

from which we see that $C_t = (P_2 - P_1) + (P_3 - P_4)/2$. Note that our derived expression for C_t does not agree with that in [28]. Our expression is in agreement with LabView VTS program calculation.

To summarize, calibration coefficients C_i, C_r, and C_t are calculated using P_1, P_2,...,P_{10} measurements according to

$$C_i = (P_{10} - P_9 + P_7 - P_8 + P_5 - P_6)/2 \tag{17}$$

$$C_r = (P_7 - P_8 - P_{10} + P_9 - P_6 + P_5)/2 \tag{18}$$

$$C_t = (P_2 - P_1) + (P_3 - P_4)/2 \tag{19}$$

where C_i, C_r, and C_t are expressed in dB and P_1, P_2,...,P_{10} are expressed in dBm.

STEP	Source	Power measured in the pit	Power measured @VTA
1	Ref-nce source	Reference source power measured with portable power meter **(P7)**	Reflected Power (Pr) measured @VTA **(P8)**
2	VTS RF source	Power out of Pi cable in the pit measured with portable power meter **(P5)**	Incident Power (Pi) measured @VTA (P6)
3	Ref-nce source	Reference source power measured with portable power meter **(P1)** (same as P7 in STEP 1)	Transmitted Power (Pt) measured @VTA **(P2)**
6	Ref-nce source	Reference source power measured with portable power meter with circulator open **(P3)**; Power reflected from transmitted power cable connection inside the dewar (circulator connected to Pt port on the top plate) **(P4)**	
8	VTS RF source		Incident Power (Pi) measured @VTA **(P9)**; Reflected Power (Pr) measured @VTA **(P10)**

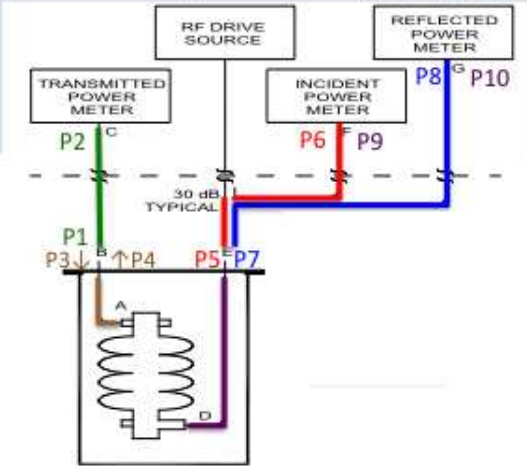

Figure 4: Cable calibrations. Calibration steps are numbered as 1, 3, 3, 6, and 8 following LabView VTS program convention described in [20]. At each step two power levels are measured, hence ten power level measurements in total. We label them as P_1, P_2,...,P_{10} following convention in [27]. Note that LabView VTS program uses a different convention. Correspondence between the two conventions is indicated in Table 2. Step number and corresponding power levels in the top part of this figure are color-coded in agreement with color-coding of the segments of VTS circuit in the diagram in the bottom part of the figure copied from [28]. For example, power levels P_1 and P_2 measured at Step 3 (indicated in green color) are used for calibrating the segment between transmitted power port connection on the top plate and transmitted power meter at the VTS stand.

Reference [27] convention	P_1	P_2	P_3	P_4	P_5	P_6	P_7	P_8	P_9	P_{10}
LabView VTS program convention	P_{10}	P_9	P_7	P_8	P_2	P_0	P_3	P_4	P_5	P_6

Table 2: Correspondence between two conventions for labeling cable calibration power level measurements.

9 Appendix B: Crystal Detector Linearity

In a typical 9-cell test (TB9NR004 VTS test in March 2012) recorded uncorrected $P_{transmitted}$ spans the range of [0.3, 40] mW ([-5, 16] dBm). For decay measurement at 3MV/m corresponding uncorrected $P_{transmitted}$ is equal to 0.5mW (-3dBm). Then we analyze $P_{transmitted}$ VTS circuit diagram [21]. Given -3dBm at $P_{transmitted}$ power meter, at the input to -30–0 dB Attenuator / 0–30 dB Amplifier signal level is 7dBm. After -30–0 dB Attenuator / 0–30 dB Amplifier attenuation consists of -2dB before the coupler through which the signal is taken to crystal detector and -30dB (coupler) + -6dB (attenuator). Finally, without any attenuation or amplification in -30–0 dB Attenuator / 0–30 dB Amplifier the signal in the crystal detector at the start of decay measurement is equal to 7dBm - 2dB - 30dB - 6dB = -31dBm which is well in the linear regime of crystal detector operation [22]. This analysis is illustrated in [23].

10 Appendix C: Sensitivity of Measured Q_0 and E_{acc} Central Values to Mismeasurements of C_i, C_r, C_t, and τ_L.

Figure 5 shows sensitivity of VTS-measured central values of Q_0 and E_{acc} to C_i, C_r, C_t, and τ_L. The sensitivity was estimated as follows:

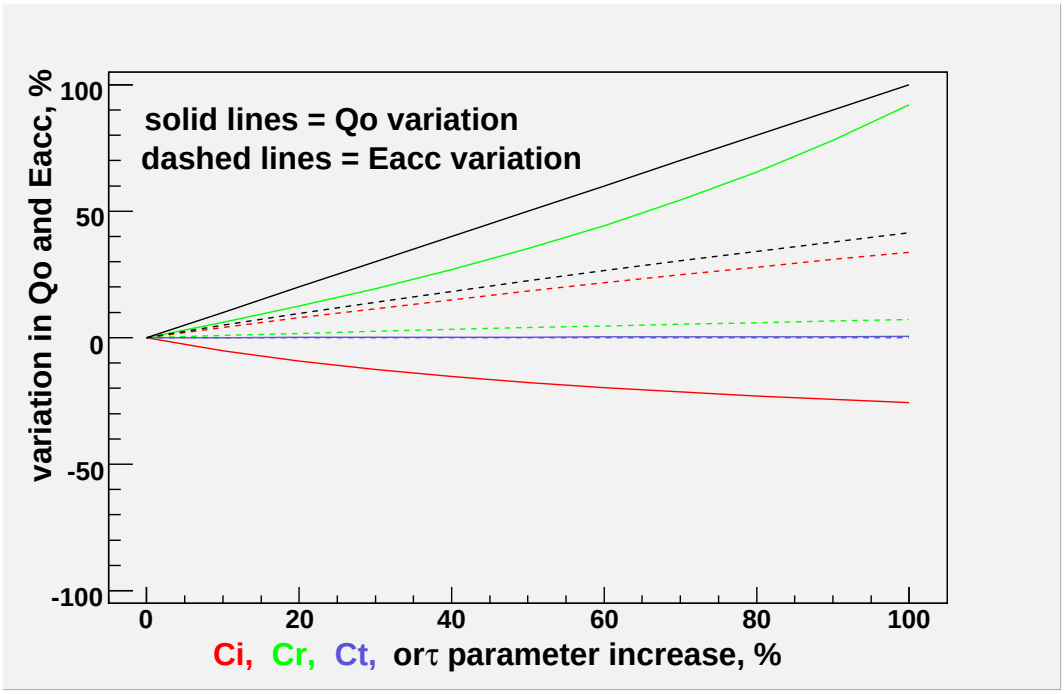

Figure 5: Q_0 (solid lines) and E_{acc} (dashed lines) variations as a function of variations in C_i, C_r, C_t, and τ_L. Red: C_i , green: C_r , blue: C_t , black: τ_L.

1. Pick a CW measured point from VTS data (TE1AES003 test on 06/08/12) : E_{acc}=5.2, Q_0=2.2.

2. With offline scripts reproduce E_{acc}=5.2 and Q_0=2.2 values using VTS data needed for their calculation (power levels, C_i, C_r, C_t, τ, frequency).

3. Increase the value of C_i and recalculate E_{acc} and Q_0.

4. Repeat previous step by varying the amount of C_i increase with respect to its value in VTS data.

5. Repeat previous two steps for C_r, C_t, and τ_L variations.

Note that in this exercise we rely on the following approximations: we neglect averaging of several decay measurements and assume that decay measurement and CW measurement are performed at the same E_{acc}. We do not expect these approximations to affect our conclusions.

Q_0 has largest sensitivity to τ_L (100% correlation between Q_0 and τ_L) and no sensitivity to C_t. Such dependencies can be easily understood from equations in Fig. 1.

τ_L dependence: Q_0 in CW calculation is linearly proportional to τ_L from decay measurement (via Q_2).

C_t dependence: C_t coefficient affects corrected value of $P_{transmitted}$. Q_0 in CW calculation depends on $P_{transmitted}$ linearly and (very weakly) via P_{loss}. Linear dependence cancels out since $Q_2 \propto 1/P_{transmitted}$ whereas dependence via P_{loss} is negligible since P_{loss} is dominated by $P_{incident}$ and $P_{reflected}$.

Q_0 sensitivity to τ_L and C_t shown in Fig. 5 would be valid for any VTS test of any cavity for any values of Q_0 and E_{acc}. In contrast, Q_0 sensitivity to C_i and C_r in Fig. 5 is specific to a given CW point in a given VTS measurement. Since Q_0 in CW measurement is inversely proportional to P_{loss}, variations in C_i and C_r may lead to strong variations in Q_0, which depend on β_1. Since Q_0 vs. E_{acc} curve, in general, is not flat, β_1 depends on E_{acc}, which varies from point to point. β_1 also depends on Q_1 which varies from cavity to cavity.

Same conclusions about E_{acc} can be made except, in general, E_{acc} dependence on C_i, C_r, and τ_L is weaker due to a square root in the CW expression for E_{acc} in Fig. 1. Sensitivity predictions discussed above were made with offline calculations relying on one picked CW point in a selected VTS test. We verified prediction of negligible C_t dependence during actual VTS test of a different cavity (SSR1-107 VTS test on 07/31/12). We artificially increased C_t by 80% and repeated both the decay measurement and CW measurement at the same input power level as before C_t modification. We found that Q_0 and E_{acc} did not change after C_t modification. If we skip the decay measurement with modified C_t, then in CW mode we measure Q_0 and E_{acc} increased by a factor of 1.8 and $\sqrt{1.8}$ respectively, as can be expected from equations in Fig. 1. These results are illustrated in Fig. 6. Establishing lack of Q_0 and E_{acc} sensitivity to C_t has practical implications: Step 3 and Step 6 of the original standard VTS calibration procedure [20] can be skipped unless there was a change in hardware configuration since previous VTS test.

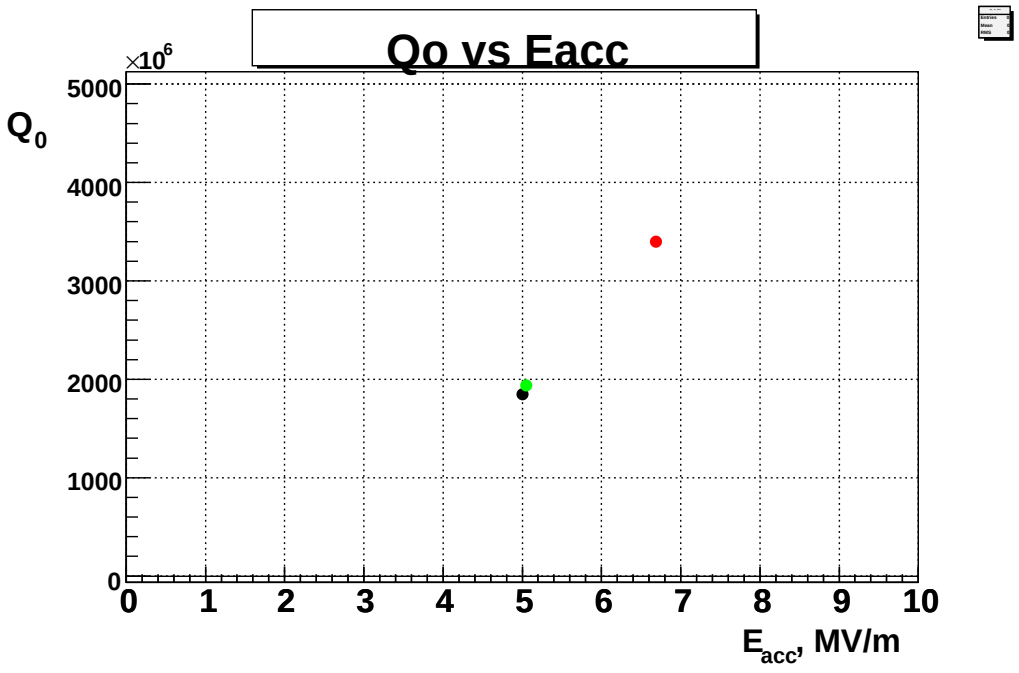

Figure 6: Verification of negligible impact of C_t on measurements of Q_0 and E_{acc}. Black: original CW reference point taken with properly calibrated C_t. Red: CW measurement after C_t increase by 80% without re-doing decay measurement i.e. still using Q_2 established with properly calibrated C_t. Green: CW after C_t increase by 80% and after decay measurement was repeated.

11 Appendix D: Averaging of Q_{ext2} Measurements

Current procedure [20] prescribes taking approximately five decay measurements and averaging central values and errors according to

$$Q_{ext2} = [Q^1_{ext2} + Q^2_{ext2} + Q^3_{ext2} + Q^4_{ext2} + Q^5_{ext2}]/5 \tag{20}$$

and

$$\sigma(Q_{ext2}) = [\sigma(Q^1_{ext2}) + \sigma(Q^2_{ext2}) + \sigma(Q^3_{ext2}) + \sigma(Q^4_{ext2}) + \sigma(Q^5_{ext2})]/5 \tag{21}$$

respectively.
From the point of view of standard error propagation rules the second formula is incorrect. Instead five errors should be added in quadrature and correlations between them should be taken into account.

However simple averaging formula turns out to be a reasonable approximation to proper error propagation as long as

1. P_{loss} and $P_{transmitted}$ errors are 100% correlated between the five decay measurements.
2. Errors on τ_L are un-correlated between the five decay measurements.
3. Errors on τ_L are a few times smaller than P_{loss} and $P_{transmitted}$ errors.

First condition is consistent with our assumptions on correlations described in Section 3. Second condition is satisfied because τ_L error of 3% is purely statistical. Third condition is also satisfied since power meter error is 4.2% and C_i, C_r, C_t errors are 15.5% , 8.9% , 6.7% respectively.

Note that error on Q_{ext2}, typically $\mathcal{O}(10\%)$ for β_1 close to 1, should be considered as an intermediate error estimate. This error cancels out to a large extent when propagated into CW measurement so that we end up with approximately 4% error on CW-measured Q_0.

12 Appendix E: Attempts to Extract Q_0 vs. E_{acc} from Decay Measurement

Decay measurement formulas in Fig. 1 suggest that Q_0 can be extracted from the decay measurement alone at E_{acc} that corresponds to maximum power. E_{acc} can be extracted from the decay measurement as well [24]. Based on our experience from VTS tests, Q_0 and E_{acc} obtained in this way are reasonably consistent with those obtained from the CW measurement. We extended this idea to extract Q_0 at several decreasing values of E_{acc} assuming that any point on the decay curve can be treated as the point at which RF power is turned off [25]. The results turned out to be inconsistent with those from the CW measurements. Possible explanation could be invalidity of the assumption that any point on the decay curve is equivalent to the point at which RF power is turned off in terms of how transmitted signal falls off from that point on.

13 Appendix F: Treatment of Correlations in VTS LabView Program

Treatment of correlations in VTS LabView program (in agreement with [**?**]) appears to be incomplete, which can be summarized as follows.

- Uncertainties on C_i, C_r, and C_t are set to constant value of 7.5% and propagated as independent uncertainties. The fact that the same power meters are used for measuring C_i, C_r, C_t and in the rest of the VTS test is not reflected in the error propagation[17].
- Same consideration applies to other sources of error that enter C_i, C_r, and C_t errors (operator error and cable losses) – they are fully correlated between decay measurement and CW measurement.
- If a variable appears several times in the calculation of error, each instance of the variable is considered to be an independent variable (error is added in quadrature each time), which leads to exaggerated total error.

[17]To be more precise, while calibration-decay correlation due to same power meters is not taken into account, decay-CW correlation is taken into account. However this is done only partially and quantitative difference it makes is very small.

References

[1] Tom Powers, Theory and Practice of RF Test Systems, Appendix A

[2] Agilent 53131A/132A 225 MHz Universal Counter Operating Guide, page XVI

[3] Agilent ESG-A/AP and ESG-D/DP RF Signal Generators Data Sheet, page 4

[4] T.Khabibouline et al, HIGH GRADIENT TESTS OF THE FERMILAB SSR1 CAVITY, IPAC2012 proceedings, WEPPC052

[5] J. Ozelis, T. Powers, Functional Description of the ILCTA-IB1 Cavity Test Stand RF, Control, and DAQ System 8/18/2006, page 3

[6] Agilent E4418B/E4419B EPM Series Power Meters, E-Series and 8480 Series Power Sensor Data Sheet, page 4

[7] Agilent E4418B/E4419B EPM Series Power Meters, E-Series and 8480 Series Power Sensor Data Sheet, page 14

[8] Agilent E4418B/E4419B EPM Series Power Meters, E-Series and 8480 Series Power Sensor Data Sheet, page 17

[9] Agilent E4418B/E4419B EPM Series Power Meters, E-Series and 8480 Series Power Sensor Data Sheet, page 3

[10] Alex Melnychuk, VTS Test Error Analysis (Part 3), presentation at Cavity Results Meeting 06/06/12, slides 15–19

[11] Tom Powers, Practical Aspects of SRF Cavity Testing and Operations, SRF Workshop 2011, slides 60-63

[12] Alex Melnychuk, VTS Test Error Analysis (Part 2), presentation at Cavity Results Meeting 05/23/12, slides 37–39

[13] Tom Powers, Practical Aspects of SRF Cavity Testing and Operations, SRF Workshop 2011, slide 37

[14] Alex Melnychuk, VTS Test Error Analysis (Part 2), presentation at Cavity Results Meeting 05/23/12, slides 41–43

[15] Alex Melnychuk, VTS Test Error Analysis (Part 2), presentation at Cavity Results Meeting 05/23/12, slides 56–58

[16] Alex Melnychuk, VTS Test Error Analysis (Part 2), presentation at Cavity Results Meeting 05/23/12, slides 59–68

[17] Timergali Khabiboulline, private communication

[18] Alex Melnychuk, VTS Test Error Analysis (Part 3), presentation at Cavity Results Meeting 06/06/12, slides 44,45

[19] http://packages.python.org/uncertainties

[20] VTS Cavity Test Procedures, Fermilab TD/T&I Department, Doc. No. TID-N-223

[21] tdserver1.fnal.gov: projects (Q):/ILCTA_VTS/RF-DAQ-Isntr/LLRF/ALTIUM CONVERSION/Imported ILCTA_VTS_LLRF_V04.PRJPCB/ILCTA_VTS_LLRF_V04.pdf

[22] Agilent 423B, 8470B, 8472B, 8473B/C Low Barrier Schottky Diode Detectors Data Sheet, page 2, Figure 6

[23] Alex Melnychuk, VTS Test Error Analysis (Part 2), presentation at Cavity Results Meeting 05/23/12, slide 54

[24] Tom Powers, Theory and Practice of RF Test Systems, page 25

[25] Alex Melnychuk, VTS Test Error Analysis (Part 3), presentation at Cavity Results Meeting 06/06/12, slides 39–43

[26] Alex Melnychuk, VTS Test Error Analysis (Part 3), presentation at Cavity Results Meeting 06/06/12, slides 50–54

[27] Tom Powers, Theory and Practice of RF Test Systems, pages 9,10

[28] Tom Powers, Theory and Practice of RF Test Systems, page 10